We are IntechOpen, the world's leading publisher of Open Access books Built by scientists, for scientists

4,800
Open access books available

122,000
International authors and editors

135M
Downloads

Our authors are among the

154
Countries delivered to

TOP 1%
most cited scientists

12.2%
Contributors from top 500 universities

CLARIVATE ANALYTICS BOOK CITATION INDEX INDEXED

WEB OF SCIENCE™

Selection of our books indexed in the Book Citation Index in Web of Science™ Core Collection (BKCI)

Interested in publishing with us?
Contact book.department@intechopen.com

Numbers displayed above are based on latest data collected.
For more information visit www.intechopen.com

8

Directed Mutagenesis in Structure Activity Studies of Neurotransmitter Transporters

Jane E. Carland, Amelia R. Edington, Amanda J. Scopelliti, Renae M. Ryan and Robert J. Vandenberg
Department of Pharmacology, The University of Sydney
Australia

1. Introduction

The delicate balance between excitation and inhibition within the central nervous system is critical to the maintenance of normal brain function. Players key to this balance are neurotransmitter transporters. Neurotransmitter transporters are drawn from two families of solute carriers (SLC), SLC1 and SLC6. The transporters for glutamate and small neutral amino acids belong to the SLC1 family, while transport of monoamines (5-hydroxytryptamine, dopamine, noradrenaline) and amino acid neurotransmitters (γ-aminobutyric acid, glycine) are mediated by members of the SLC6 family. These integral membrane proteins regulate the concentration of neurotransmitters, such as glutamate and glycine, within the synapse. They utilise pre-existing electrochemical gradients to drive the transport of neurotransmitters across neuronal and glial membranes, terminating neurotransmission and replenishing intracellular levels of neurotransmitter for future release. Neurotransmitter transporters are targeted by a number of substances, both therapeutic (antidepressants, anticonvulsant, antipsychotics, analgesics, anxiolytics) and addictive (cocaine, methampetamine). Their dysfunction is associated with multiple disorders, including epilepsy, ischaemic stroke, neuropathic pain and schizophrenia (Dohi et al., 2009; Sur & Kinney, 2004). Thus, structure activity studies of transporters are essential to provide new insights into their function and direct the design of novel, transporter-specific therapeutics.

Since the cloning of the GABA transporter, GAT1, in 1990 (Guastella et al., 1990), directed mutagenesis studies have underpinned our understanding of the secondary structure and function of neurotransmitter transporters. This work has subsequently been supported, and significantly advanced, by the high resolution crystal structures of prokaryotic homologues of the SLC1 and SLC6 families. The crystal structure of the SLC1 homologue from *Pyrococcus horikoshii* (Glt_{Ph}) was the first to be solved at 3.5 Å resolution (Fig 1A) (Yernool et al., 2004). This was followed in 2005 by the crystal structure of a homologue of the SLC6 family from *Aquifex aeolicus (*$LeuT_{Aa}$) at 1.65 Å resolution (Yamashita et al., 2005) (Fig 3A). These crystal structures have provided important insights into the interactions of transporters with substrates, ions, lipids and inhibitors, allowing the postulation of numerous functional mechanisms. However, the details provided by these high-resolution structures are insufficient to fully understand transport mechanisms. The knowledge obtained from

crystal structures and 3D models can be used to direct mutagenesis work (utilising chimeric transporters and site-directed mutagenesis), electrophysiology and uptake studies to determine the molecular basis for transporter function. The techniques described in this chapter can be applied to other membrane proteins, such as G-protein coupled receptors and ligand-gated ion channels.

1.1 The SLC1 family of transporters

The SLC1 family of neurotransmitter transporters includes five human excitatory amino acid transporters (EAAT1 to EAAT5) (Slotboom et al., 1999) and two neutral amino acid transporters (ASCT1 and ASCT2) (Arriza et al., 1993; Kanai & Hediger, 2004). The EAATs exhibit 40-44% sequence identity with ASCTs and approximately 36% sequence identity with the related Na^+-coupled aspartate transporter, Glt_{Ph} (Fig. 2). The high resolution crystal structure of Glt_{Ph} reveals that SLC1 transporters exist as bowl-shaped trimers (Fig. 1A) (Yernool et al., 2004). Each protomer is comprised of eight transmembrane domains (TM1-8) and two re-entrant hairpin loops (HP1 and HP2). TM1, TM2, TM4, and TM5 mediate intersubunit contacts and support the "transport" domain, which is composed of TM3, TM6, TM7, TM8, HP1 and HP2 (Fig. 1B). This transport domain mediates substrate and ion translocation, and each protomer has an independent translocation pathway.

The EAATs are critical components of excitatory synapses, where they mediate the high affinity uptake of the dominant excitatory neurotransmitter, glutamate, as well as L- and D-aspartate. Both EAAT1 and EAAT2 are expressed in glia. Of these two subtypes, EAAT2 is the more widely distributed and is the major regulator of glutamate concentrations in the central nervous system. EAAT3 is expressed on neuronal membranes throughout the brain, while EAAT4 is selectively expressed on cerebellar Purkinje cells. EAAT5 is expressed on retinal neurons. Glutamate uptake is coupled to the co-transport of three Na^+ ions and one H^+ and the counter-transport of one K^+ ion, rendering them electrogenic (Zerangue & Kavanaugh, 1996). In addition, glutamate transport is associated with a thermodynamically uncoupled Cl^- conductance (Fig. 1C) (Fairman et al., 1995, Wadiche et al., 1995).

1.2 The SLC6 family of transporters

Members of the SLC6 transporter family are responsible for the transport of monoamine (dopamine, serotonin/5-hydroxytryptamine, noradrenaline) and amino acid (GABA and glycine) neurotransmitters across cell membranes. Two glycine transporters (GLYT1 and GLYT2) have been cloned, and five GLYT1 splice variants (GLYT1a to GLYT1e) and three GlyT2 splice variants (GLYT2a to GLYT2c) have been identified. The crystal structure of the prokaryotic transporter $LeuT_{Aa}$ serves as a useful template for unravelling the functional implications of transporter structures (FIG. 3). Members of the SLC6 family are traditionally thought to exist as monomers (Horiuchi et al., 2001; Lopez-Corcuera et al., 1993), although more recent work suggests that they may form dimers *in vivo* (Bartholomaus et al., 2008). Each subunit is formed by twelve transmembrane domains (TM1-12), with amino- and carboxy-termini located on the intracellular side of the membrane. Each subunit exhibits a two-fold axis of symmetry, with TM1 to TM5 corresponding to TM6 to TM10 with an inverted topology repeat. TM1 to TM10 form the core of the transporter, with TM1 and TM6 exhibiting the highest degree of sequence homology. They run antiparallel and exist with a central unwound section. The area surrounding this central unwound section is critical for substrate and ion binding.

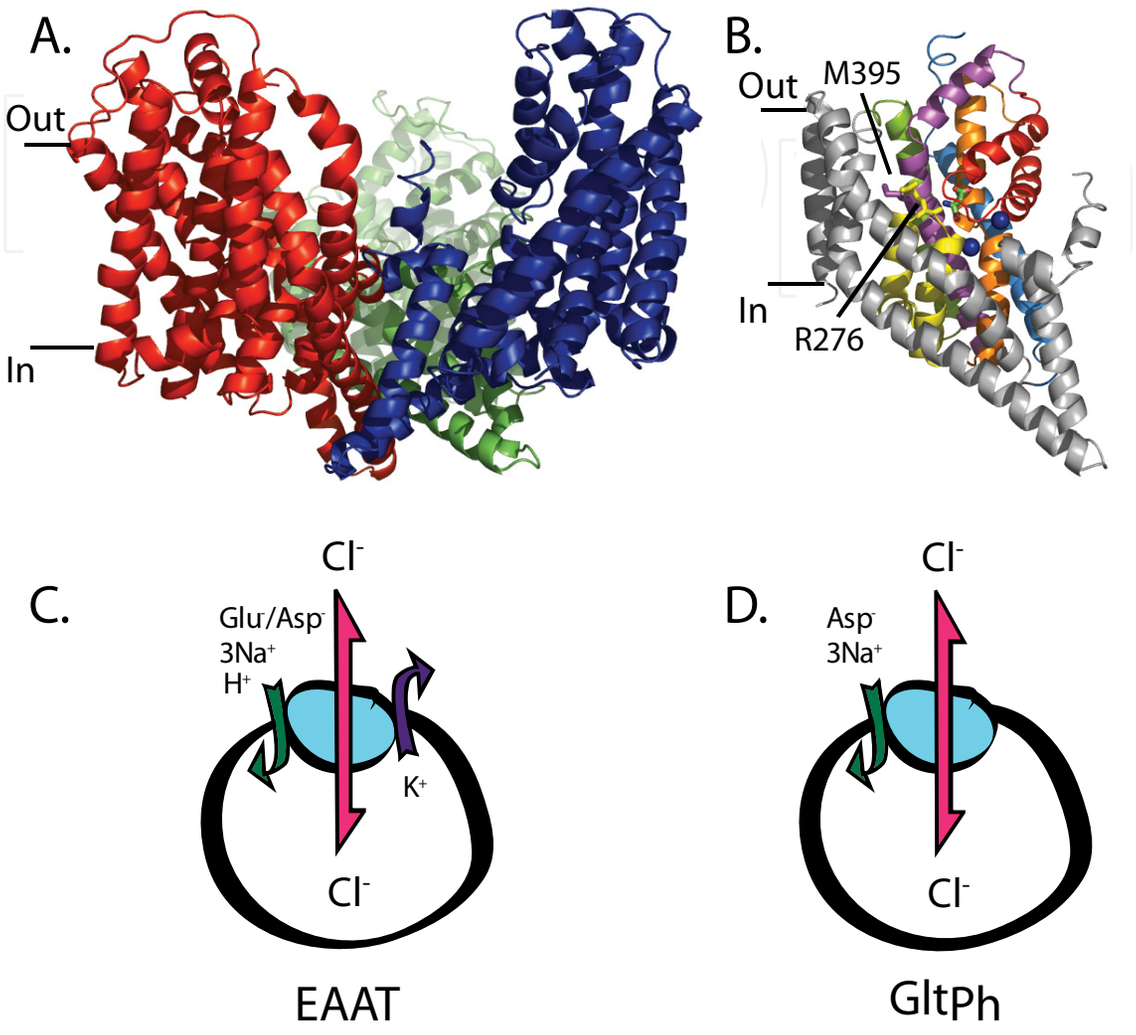

Fig. 1. The crystal structure of the prokaryotic transporter Glt_{Ph} and the stoichiometry of transport by the excitatory amino acid transporters (EAAT1- EAAT5) and Glt_{Ph}. A. Glt_{Ph} is a bowl shaped trimer viewed in the plane of the membrane. Individual protomers are coloured red, green and blue. B. A single protomer of the Glt_{Ph} trimer (PDB 2NWX). The C-terminal domain is shown in colour; HP1 (yellow), TM7 (orange), HP2 (red) and TM8 (magenta). Bound aspartate is shown in stick representation and two Na^+ ions are shown as blue spheres. R276 (HP1) and M395 (TM8), which are discussed in section 3.5, are also shown in stick representation. Structures were viewed and rendered in PyMOL (http://www.pymol.org) (Schrodinger, 2010). C. Glutamate or aspartate transport via the EAATs is coupled to three Na^+ ions and one H^+, followed by the counter-transport of one K^+ ion. Binding of Na^+ and substrate to the EAATs activates a thermodynamically uncoupled Cl^- conductance (*pink arrow*). D. Aspartate transport via Glt_{Ph} is coupled to the co-transport of three Na^+ ions, but is not coupled to the movement of either H^+ or K^+ ions. Na^+ and aspartate binding to Glt_{Ph} also activates an uncoupled Cl^- conductance (*pink arrow*).

Fig. 2. Amino acid sequence alignment of SLC1 family members. Sequences for EAAT1-3, ASCT1 and Glt_{Ph} are shown. Transmembrane domains are indicated using the colour scheme as for the structure of Glt_{Ph} in Fig. 1. Homologous regions are highlighted in black. Residues highlighted in red boxes with yellow background are discussed in the text. The blue line (connecting Q93 to V452 in EAAT1) indicates that cysteine mutants of these two residues can be cross-linked (see section 3.4 for details).

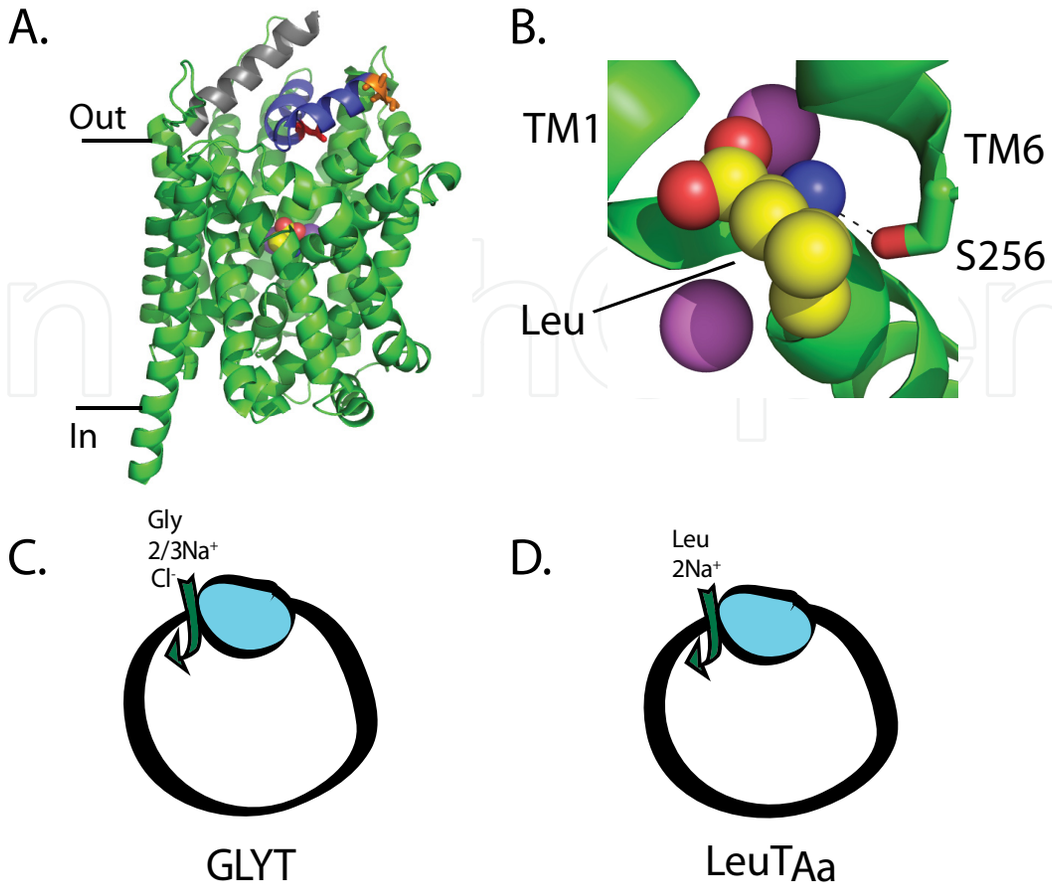

Fig. 3. The crystal structure of the prokaryotic transporter $LeuT_{Aa}$ and the stoichiometry of transport by the GLYTs and $LeuT_{Aa}$. A. The structure of $LeuT_{Aa}$ viewed in the plane of the membrane (PDB 2A65). Bound leucine is shown in A space-filling representation, and the 2 Na^+ ions are shown as purple spheres. Extracellular loop 2 (EL2, grey) and extracellular loop 4 (EL4, blue) are highlighted (see section 2.2 for details). EL4 residues R531 and K532 (orange stick representation) and I545 (red stick representation) are also highlighted (see section 3.2 for discussion). B. Bound leucine interacts with transmembrane domains TM1 and TM6. The hydrogen bond between the nitrogen atom of leucine and the side chain of serine 265 is represented by a dashed line (see section 3.2 for details). Na^+ ions are shown as purple spheres. C. Glycine transport via the GLYTs is coupled to two (GLYT1) or three (GLYT2) Na^+ ions and one Cl^- ion. D. Alanine transport via $LeuT_{Aa}$ is coupled to the co-transport of two Na^+ ions.

Mammalian members of the SLC6 family share 20-25% sequence identity with the prokaryotic transporter $LeuT_{Aa}$ (FIG. 4). GLYT1 and GLYT2 are structurally similar and exhibit 48% sequence homology (FIG. 4), but they display significant functional differences. GLYT1 is predominantly expressed in glia at excitatory glutamatergic synapses, where they are responsible for regulating glycine, which acts as a co-agonist at NMDA receptors. Of the five GLYT1 isomers identified, GLYT1b and GLYT1c are nervous system-specific. In contrast, GLYT2 is typically localized with glycine receptors at inhibitory glycinergic synapses (spinal cord). The translocation of glycine by both transporters is coupled to the co-transport of Na^+ and Cl^- (FIG. 3), but the stoichiometry of ion-flux coupling by GLYT1 and GLYT2 differs. The transport of one glycine molecule is coupled to the co-transport of

two Na^+ ions and one Cl^- ion for GLYT1 transporters, while the movement of three Na^+ ions and one Cl^- ion is coupled to glycine transport for GLYT2 (Fig. 3C).

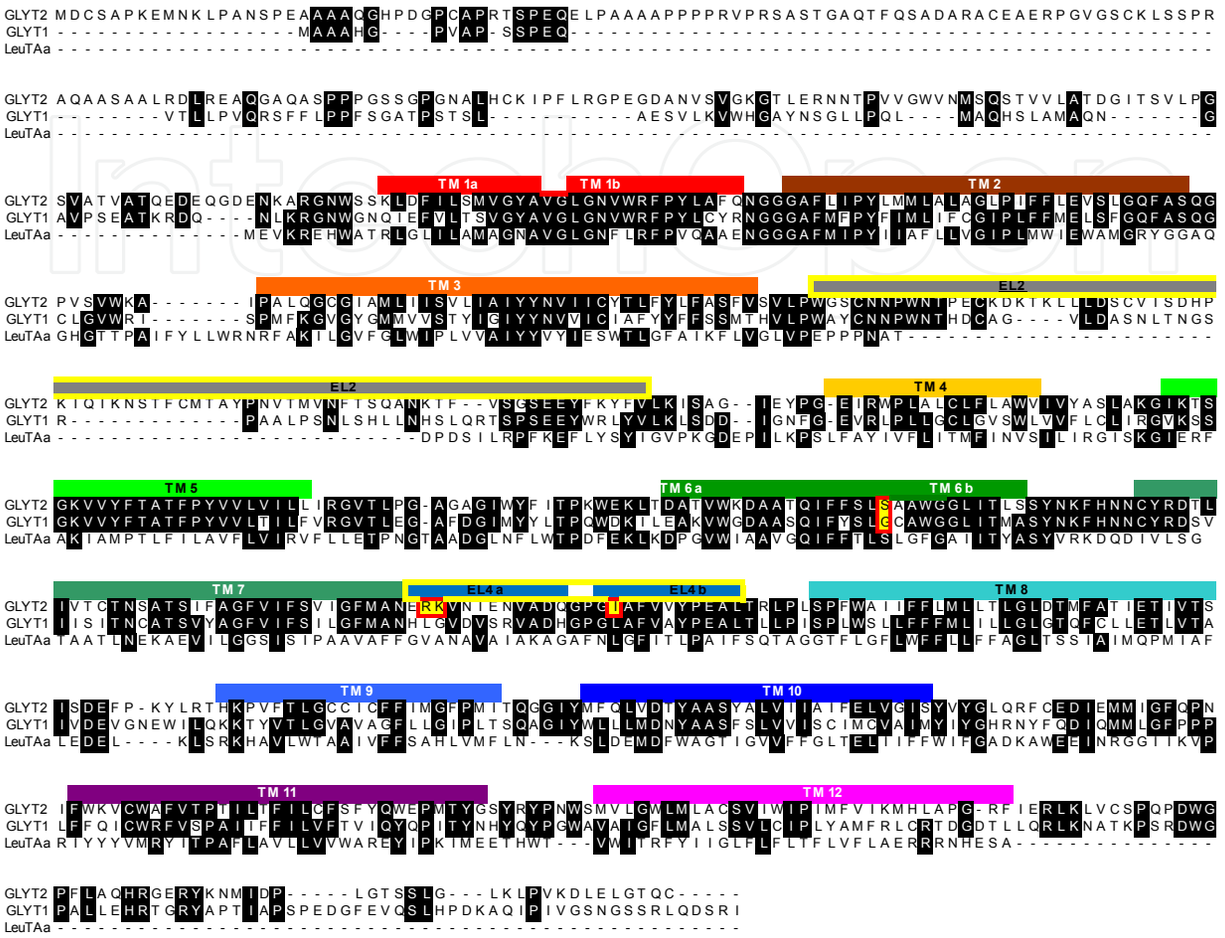

Fig. 4. Amino acid sequence alignment of GLYT1, GLYT2 and $LeuT_{Aa}$. Transmembrane domains are indicated using the colour scheme used for the structure of $LeuT_{Aa}$. Homologous regions are highlighted in black. Chimeric transporters were generated between GLYT1 and GLYT2 in which extracellular loops 2 and 4 (highlighted with yellow edges) were switched between the two transporters (see section 2.2 for details). Residues highlighted in red boxes with yellow background are discussed in the text.

2. The use of chimeras in studies of neurotransmitter transporters

Chimeras provide an excellent tool for the study of neurotransmitter transporters. Switching specific regions/structures between transporters can provide insights into transporter function and substrate selectivity and inform the design of directed mutagenesis studies. Further, chimeras between mammalian and bacterial transporters have the potential to assist with the crystallisation of transporters, thereby facilitating the determination of the structure of mammalian transporters. We employ a fusion PCR technique to create chimeric junctions at specific amino acid locations, allowing for the precise design of chimeras. We have produced numerous chimeras using this method, including chimeras of GLYT1 and GLYT2.

2.1 PCR fusion methodology

Conventional chimera construction methodology relies on restriction enzyme cloning, in which unique restriction enzyme sites are introduced into both the acceptor and the donor proteins. While this technique allows for the production of chimeras with specific/known junction points, the availability of unique restriction enzyme sites can impose limitations on the design of potential chimeras. In contrast, the PCR fusion technique (Shevchuk et al., 2004) creates chimeric junctions at any amino acid, without the need for restriction enzyme sites. In this method (Fig. 5), each segment of the final chimera is amplified in individual PCR reactions. The primers are designed to engineer complementary overlapping sequences onto the junction-forming ends of each product. The PCR primers possess typical properties (18-24 nucleotides in length and a melting temperature of ~64ºC). The overlapping sequences correspond to the desired chimeric junction sites between subunits. The strands of the PCR products (duplex DNAs) are routinely separated and allowed to reanneal by cycles of heating and cooling. A partially duplex chimera can form as a result of annealing by the complementary regions of different fragments, one half of the chimeras will have free 3′-ends that can be elongated by DNA polymerase. The other half will have free 5′-ends that cannot be elongated. If more than two PCR products are involved, eventually a full-length chimera forms. The resulting duplex chimera is then amplified by PCR with oligonucleotide primers containing restriction enzyme sites at the 5′ and 3′ ends of the DNA of the chimera to facilitate subcloning into a suitable vector. For chimeras that require more than three fragments, it is often best to produce an initial chimera of three fragments and then incorporate additional fragments as required. It is important to obtain complete DNA sequences of any clones generated in this manner to confirm the junction sites and also to ensure that there have been no spurious sequence changes.

2.2 Identifying determinants of drug selectivity

Drugs that have selective effects *in vivo* are much sought after. Such compounds potentially have minimal side effects, making them attractive options as therapeutics. Studies suggest that the GLYTs may provide a novel therapeutic target for the development of drugs to treat neurological disorders and pain. In particular, GLYT1 is considered a potential target for the development of agents to treat schizophrenia (Sur et al., 2004). GLYT2 is a key target for studies to develop molecules to treat chronic pain (Aragon & Lopez-Corcuera, 2003). *N*-Arachidonylglycine (NAGly) is an endogenous derivative of arachidonic acid. NAGly has been shown to induce analgesia in rat models of neuropathic and inflammatory pain (Succar et al., 2007; Vuong et al., 2008). One of the mechanisms of action of NAGly is the inhibition of GLYT2 (IC_{30} = 3 μM), whilst it has no effect on GLYT1 (Wiles et al., 2006). Understanding the molecular basis of NAGly selectivity may aid in the development of novel analgesic compounds.

Extracellular loops EL2 and EL4 have been implicated in mediating inhibition of the GLYTs. Residues that contribute to the binding site of Zn^{2+}, a non-competitive inhibitor of GLYT1, have been identified in EL2 and EL4 (Ju et al., 2004). Zn^{2+} has been proposed to inhibit GLYT1 by binding to EL2 and EL4, restricting the movement of these loops and thus preventing glycine transport. $LeuT_{Aa}$, the bacterial homologue of the GLYTs, has been crystallized in the presence of clomipramine, a non-competitive inhibitor (Singh et al., 2007), and tryptophan, a competitive inhibitor (Singh et al., 2008). Clomipramine was shown to

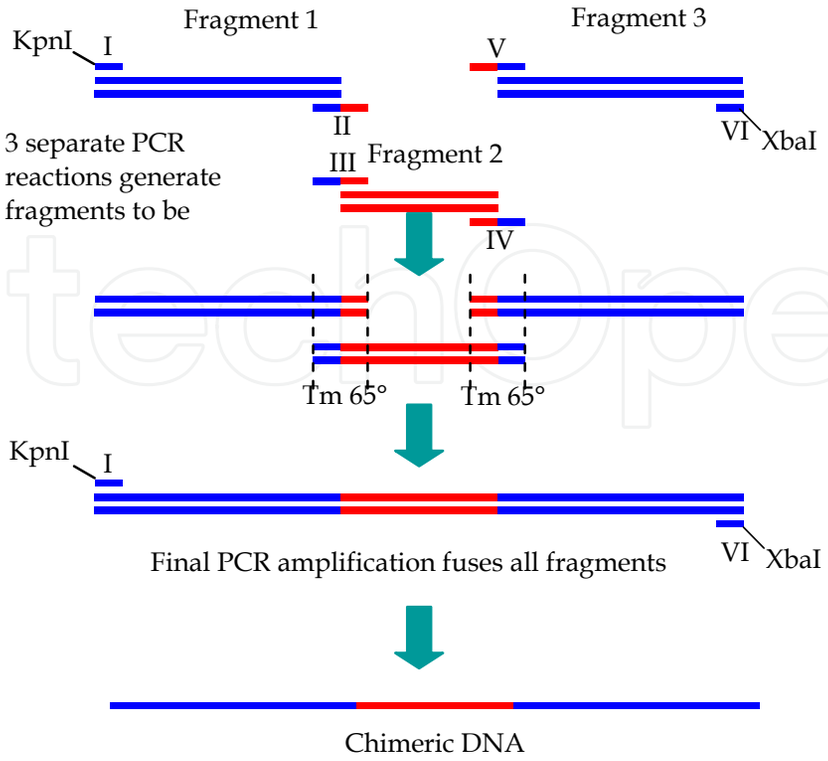

Fig. 5. A schematic summary of the construction of chimera GLYT1(EL2) using the PCR fusion methodology. The DNA sequence of the donor cDNA (GLYT1) is in blue and the acceptor cDNA (GLYT2) is in red. cDNAs of GLYT1 and GLYT2 in the presence of their corresponding primers (I and II, III and IV, V and VI) undergo PCR to generate three fragments with the appropriate homologous ends. The fragments are 'fused' together in another reaction, in which the single strands from the overlapping regions serve as internal primers (see text). The final PCR amplification reaction fuses ('zips') all the fragments in the presence of primers I and VI, which, in this case, include restriction site for the enzymes *Kpn*I and *Xba*I. The final product is the chimera GLYT1(EL2) with two unique restriction sites engineered on either end to allow for insertion of the chimeric gene into the vector pOTV. The restriction sites may be altered for subcloning into different vectors.

stabilize $LeuT_{Aa}$ in an occluded state by interacting with a number of transmembrane domains and displacing the tip of EL4. In contrast, the presence of the competitive inhibitor tryptophan appeared to trap the transporter in an open-to-out conformation. Four separate tryptophan molecules were identified in this crystal structure, with one of them found to be interacting with EL2 and EL4. These observations suggest that these loops play key roles in the inhibition of GLYTs.

In order to ascertain the molecular basis for the inhibitory activity of NAGly on GLYT2, chimeras were generated between GLYT1 and GLYT2, in which EL2 and/or EL4 were switched (Fig. 6). A chimera is named according to its parental transporter, with the inserted loop in parentheses. For example, GLYT2(EL2) is predominantly GLYT2 with the EL2 of GLYT1. One of the important controls required when using a chimeric protein to understand structure-function relationships is the ability to maintain the functional properties of the chimera. For chimeras that are predominantly GLYT2, the EC_{50} for glycine

was very similar to that of the parental GLYT2 transporter, which indicates that these chimeras transport glycine similar to GLYT2. With the GLYT1-based chimeras, GLYT1(EL2) and GLYT1(EL2, EL4), the EC_{50} for glycine was increased by 6-8 fold compared to GLYT1. Thus, for the GLYT1-based chimeras, the transport of glycine differs slightly from the parent transporter; and, therefore, we are not able to be as confident that other functional changes are solely due to the region of interest. Nevertheless, the experiments using the GLYT2-based chimeras yielded valuable information concerning the domains responsible for NAGly sensitivity. GLYT2 is inhibited by NAGly, whereas GLYT2(EL2) and GLYT2(EL4) have reduced sensitivity (Edington et al., 2009). These observations suggest that EL2 and EL4 contribute to forming an inhibitory site on GLYT2.

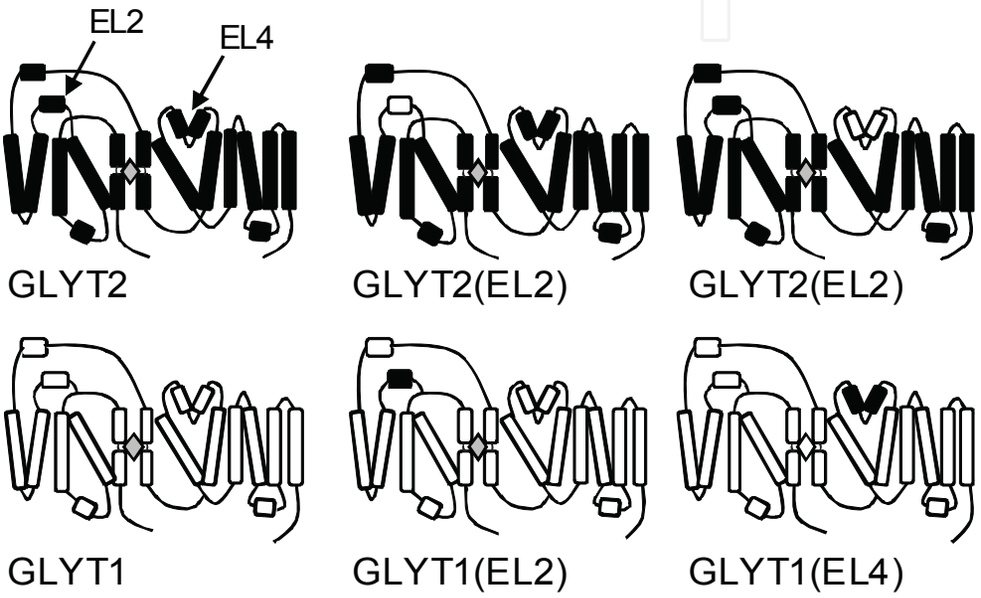

Fig. 6. A schematic diagram of the topology of the wild-type transporters GLYT2 and GLYT1 and their EL2 and EL4 chimeras. *Black* indicates the regions of the transporter from GLYT2 and *white* indicates the regions from GLYT1. Shown are GLYT2, GLYT2(EL2), GLYT2(EL4), GLYT1, GLYT1(EL2), and GLYT1(EL4).

3. Site-directed mutagenesis

Identifying domains that are responsible for conferring functional differences between transporters is only the first step in understanding the molecular processes that dictate neurotransmitter transporter function. Chimeric and directed mutagenesis studies are mutually beneficial and, when used in conjunction, can increase the efficiency and efficacy of experimentation. Information obtained in the study of chimeric transporters helps to focus site-directed mutagenesis studies to specific domains. The introduction of point mutations within these regions can then provide very useful information about the function of specific residues and the location of substrate and ion binding sites. Conventional mutagenesis studies utilise amino acid sequence alignments between multiple members of a transporter family to direct and design mutagenesis studies. However, this work often relies on the mutation knocking out a particular function and thereby assigning that function to the residue of interest. This approach can generate misleading conclusions because loss of function can be the result of a number of changes, many of which do not necessarily reflect a

direct disruption of the interaction being investigated. To avoid this issue, we employ knowledge obtained from recent advances in high resolution transporter crystal structures and homology models to improve our accuracy in predicting residues of interest and successfully creating functional mutants. Crystal structures provide a powerful 3-dimensional tool that enables us to visualise each residue and their individual contacts with the substrate/ions/other residues, thus improving the selection process. In addition, homology models provide a computational prediction of the global effect of a mutation. Thus, they can be used to predict which mutations will be accommodated by individual transporters. We have undertaken numerous mutagenesis studies that have, among other things, identified the glycine substrate binding site in GLYT1 and GLYT2, helped to characterise selective drug-binding sites on the GLYTs and clarified the specificity of ion and substrate interactions with the EAATs and Glt_{Ph}.

3.1 Directed mutagenesis methodology

Site-directed mutagenesis is a powerful tool that makes select changes to the genetic code of a protein to alter the amino acid sequence. The resultant mutant protein exhibits subtle structural changes. The ability to selectively manipulate amino acids in a controlled manner provides a powerful tool that is exploited by researchers undertaking structure-function studies. It should be noted that the importance of loss of function mutants must be interpreted with caution. Disruption of transport functions following a mutation can result in loss of function. However, loss of function could also result from misfolding of a protein or altered expression levels. Therefore, mutants that lose function are only useful if the cause of loss of function can be accurately ascertained.

Site-directed mutagenesis involves the use of specifically designed primers (sense and antisense) that include a point mutation of interest in the centre of the sequence. Each primer is 18-24 nucleotides in length with a melting temperature of ~64°C. The primers incorporate the mutation into an intronless gene, using the cDNA as template in a PCR reaction, with the elongation by DNA polymerase. Following amplification, the endonuclease *Dpn*I, which recognizes methylated and hemimethylated DNA, can be added to the amplification reaction to digest the parental cDNA. It is important to obtain DNA sequences to confirm the mutation. The mutant DNA is subcloned into the appropriate vector. In the studies we describe, the Oocyte Transcription Vector (pOTV) is used, as it enables efficient RNA production and facilitates high expression levels of protein in *Xenopus laevis* oocytes. To construct a double point mutation, one set of primers may be used when the two residues are next to each other or in close proximity. However, if the two mutations are further apart, DNA encoding one mutation is initially made and used as the template for the second mutation. Site-directed mutagenesis kits are sold by many companies (e.g., Stratagene, Promega, Clonetech). We routinely use the QUIKCHANGE(tm) Site-Directed Mutagenesis kit from Stratagene.

3.2 Mutagenesis to identify determinants of drug selectivity of glycine transporters

The use of chimeric GLYT transporters allowed the identification of EL2 and EL4 as being regions critical for determining the selective activity of NAGly on GLYT2 (Edington et al., 2009). Having identified the regions of interest, we used site-directed mutagenesis to identify the residues within these regions that form the selective drug-binding site. Our

chimeric study (see Section 2.2) revealed that NAGly interacted with EL4, so the aim of the subsequent mutagenesis study was to identify the key residues in EL4 that play a role in determining the differential sensitivity of GLYT2 compared to GLYT1.

The EL4 of GLYT2 exhibits 60% sequence identity with the GLYT1 EL4. Point mutations were introduced at all positions within the GLYT2 EL4 that differed from GLYT1. In total, eleven mutations were produced. Each resulted in a functional mutant GLYT2 transporter that exhibited glycine transport unchanged from that of the wild-type transporter. Three mutations resulted in changes in sensitivity to NAGly. Mutation of arginine at position 531 to leucine (R531L) and lysine at position 532 to glycine (K532G) resulted in modest reductions in NAGly sensitivity (IC_{30} = 13 ± 2 μM and 9 ± 1 μM, respectively) compared to GLYT2 (IC_{30} = 3.4 ± 0.6 μM). In contrast, the mutation of isoleucine at position 545 to leucine (I545L) markedly reduced NAGly sensitivity (IC_{30}>30μM) (Edington et al., 2009).

This work revealed that three residues within EL4 are critical to the inhibitory activity of NAGly on GLYT2. Modelling studies place I545 in the middle of EL4, while R531 and K532 are located at the edge of EL4. It is surprising that a conservative mutation at position 545 (an isoleucine to a leucine) would have the most dramatic impact. Two likely possibilities follow. (1) NAGly may bind to I545, and the I545L mutation may distort the way that NAGly fits into the binding site. (2) The I545L mutation may alter the conformation of the two arms of EL4, which then impacts on the way that this domain interacts with other elements that may be crucial for NAGly binding. The carboxyl groups of NAGly may interact with the positively charged R531 and K532 residues. Further structural studies are required to fully characterize the specific interaction sites between the NAGly and GLYT2.

3.3 Substrate selectivity of the GLYTs

GLYT1 and GLYT2 can be differentiated by their substrate selectivity and inhibitor sensitivity. GLYT1 transports both glycine and the N-methyl derivative of glycine, sarcosine, while GLYT2 only transports glycine (Supplisson & Bergman, 1997). In addition, GLYT1 is selectively inhibited by *N*[3-(4-fluorophenyl)-3-(4'-phenylphenoxy) propylsarcosine (NFPS) (Aubrey & Vandenberg, 2001). The crystal structure of $LeuT_{Aa}$ provides a good working model for the study of GLYTs. As with the GLYTs, the substrate binding site of $LeuT_{Aa}$ is formed at the junction between TM1–5 and TM6–10. It is composed of amino acid residues from TM1 and TM6 (Yamashita et al., 2005). Both of these transmembrane domains contain an unwound segment, and many of the substrate contact sites are with the main chain atoms of these unwound segments. Sequence alignments between $LeuT_{Aa}$ and the GLYTs revealed that there are a number of identical residues and some key differences in the predicted substrate binding site. In particular, in the crystal structure of $LeuT_{Aa}$, the amino group of leucine is hydrogen-bonded to the hydroxyl group of the side chain of serine at position 256 (Fig 3B). This residue is located in TM6. We focused on the role of the corresponding residues in GLYT1b and GLYT2a to investigate if this residue is a determinant of GLYT substrate selectivity (Vandenberg et al., 2007).

Serine at position 256 in $LeuT_{Aa}$ corresponds to a glycine residue (G305) in GLYT1b and a serine residue (S481) in GlyT2a. The G305 in GLYT1b was mutated to a serine (GLYT1-G305S) and S481 in GLYT2a was mutated to a glycine (GLYT2-S481G) using site directed mutagenesis (Vandenberg et al., 2007). In contrast to wild type GLYT2a, sarcosine is a

substrate of the GLYT2a-S481G mutant. The maximal current (97 ± 2%) and EC_{50} (26.2 ± 1.3 μM) of sarcosine at the mutant receptor are similar to that for wild-type GLYT1b (87 ± 1%, 22 ± 1 μM). The introduction of the corresponding mutation, G305S, into GLYT1b reduced levels of surface expression to approximately 10% of wild type. To overcome this limitation, two additional mutants were generated, GLYT1b-G305A and GLYT2a-S481A. Glycine transport of both mutant receptors is similar to that of wild type. However, incorporation of the S481A substitution into GLYT2a produced a transporter that could transport sarcosine with an efficacy similar to that of GLYT1b (70 ± 3%), but with a reduced affinity (590 ± 50 μM) relative to wild type. Combined, these findings demonstrate that residues at this position are important for sarcosine transport. For GLYT2a, sarcosine can be transported if an alanine or a glycine residue is present at this site, but not if a serine residue is present.

3.4 Mutagenesis to identify transport and channel domains of glutamate transporters

Glutamate transporters have two distinct functions: ion coupled glutamate transport and glutamate-activated chloride channel activity. In 1995, two studies demonstrated that the two functions co-exist in the same protein (Fairman et al., 1995; Wadiche et al., 1995). Glutamate binding is required for activation of the channel, but the direction of Cl^- ion flow through the channel domain is uncoupled from the direction of glutamate transport. This raised the question as to how the protein could support the dual functions. In the following section, we will describe how mutagenesis has been used to understand the structural basis for the dual functions of glutamate transporters. This is an interesting example of the complementary nature of mutagenesis and crystallography approaches to understand the functional properties of this class of transporters.

Prior to the determination of the crystal structure of Glt_{Ph}, mutagenesis was used to identify residues that may play a role in transporter function. Valine 452 (V452) of EAAT1 is located in the HP2 domain, and the V452C mutation does not alter the functional properties of the transporter. After modification of the V452C mutant with the methanethiosulfonate (MTS) reagent, [2-(trimethylammonium)ethyl] methanethiosulfonate (MTSET), the protein is no longer capable of transporting glutamate; but it still retains the glutamate-activated chloride channel (Ryan & Vandenberg, 2002). This suggests that the two functions are mediated by distinct conformational states of the transporter. In a separate study, our group attempted to identify regions of the transporter that form the chloride channel. We focussed our mutagenesis studies on TM2. TM2 contains a number of positively charged residues at the extracellular edge of the helix and a number of uncharged serine and threonine residues in the middle of the helix. We postulated that positive charges at the extracellular edge would attract anions into the channel and the hydrophilic residues within the channel would facilitate anion movement through the channel. To address this hypothesis, we mutated the positively charged residues at the extracellular edge to cysteine residues and probed the reactivity of the cysteine residues to both positively and negatively charged MTS reagents. The negatively charged MTS reagents had faster rates of reactivity than the positively charged MTS reagents, which suggested that the positively charged residues do attract negative charges to the extracellular edge of TM2. Substitutions of the hydrophilic serine and threonine residues in the middle of TM2 to small aliphatic residues significantly altered the anion permeability of the channel without affecting the transport function. This confirmed that the two functional properties of the transporter are mediated by separate

domains and also that the serine and threonine residues are likely to line the pore of the channel.

The studies described above were carried out prior to any knowledge of the three dimensional structure of the transporter, and so we attempted to identify how close the channel domain was from various other sites on the transporter by cross-linking experiments. Cysteine residues were introduced within TM2 and then at various other sites of the transporter, including V452 (see above). A disulfide bond formed spontaneously between V452C (in HP2) and Q93C (in TM2), indicating that these two residues must come into close proximity. From this study a crude structural model for these parts of the transporter was developed (Fig. 7A).

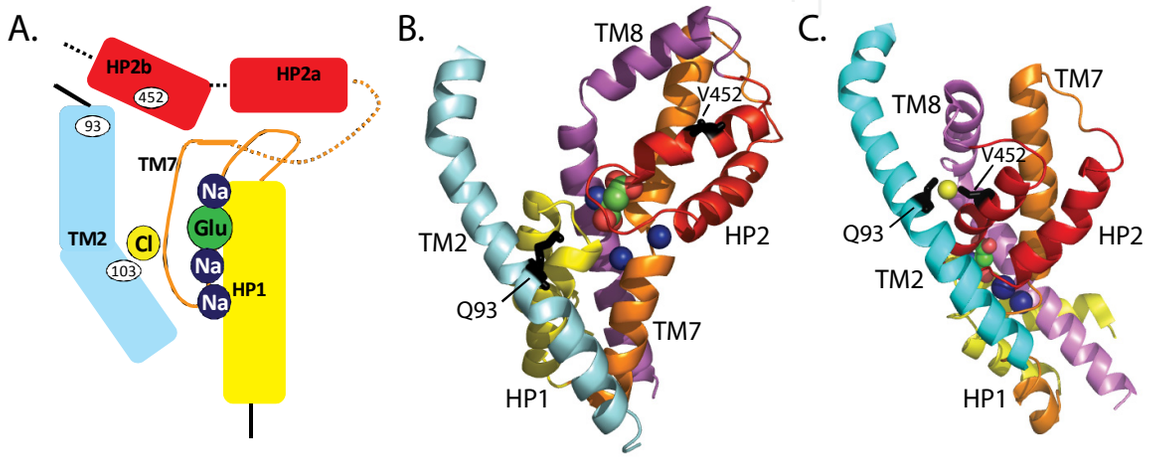

Fig. 7. Structural predictions of the relationship between the glutamate binding and translocation domain and the chloride conducting domain. A. A structural model for glutamate transport and Cl^- ion permeation of EAAT1. We have omitted the K^+ ion and H^+ for simplicity. The *thick line* is in the plane of the paper and the *dashed line* is behind the plane of the paper. V452C can form a disulfide bond with Q93C. We propose that Cl^- ions interact with residues along TM2. In this model, we suggest that glutamate and Na^+ ions permeate the same pore as Cl^- ions, but that there are separate molecular determinants for the two functions. B, C. The structure of the transport domain composed of HP1 (yellow), TM7 (orange), HP2 (red) and TM8 (purple) relative to TM2, which contains molecular determinants for Cl^- permeation. Bound aspartate is shown in space-filling representation, and two Na+ ions are represented as blue spheres. The residues equivalent to Q93 and V452 are in stick representation and coloured black. B. Shows the distance between Q93 and V452 in the occluded state (PDB 2NWX), while C is the Hg^{2+} cross-linked structure showing the conformational changes required to bring Q93 and V452 into close proximity (PDB 3KBC, Hg^{2+} shown as a yellow sphere).

The crystal structure of Glt_{Ph} was published in late 2004 (see above for a description of the structure); and, whilst the structure revealed many important details about substrate binding, the nature of the mechanism of activation of the chloride channel was not clear. The equivalent residues to V452 and Q93 in Glt_{Ph} are approximately 20 Å apart (Fig. 7B, equivalent residues in a Glt_{Ph} protomer are represented in black), which suggested that these residues were unlikely to come sufficiently close to form a disulfide bond. The first step in resolving this apparent contradiction came from confirming that hydrophilic

residues in TM2 of Glt_{Ph} also form part of the lining of the chloride channel lumen, as observed for EAAT1 (Ryan & Mindell, 2007). The laboratory of Olga Boudker then repeated the crosslinking experiments in Glt_{Ph}, using cysteine mutants and adopting a similar approach to the one our group had done for EAAT1. Whilst spontaneous disulfide bonds did not form between the two residues in Glt_{Ph}, it was possible to catalyse the formation of a bond between the two cysteine residues using Hg^{2+}. It was concluded that the two domains can indeed move sufficiently to allow the two residues to come into close proximity. The cross-linked Glt_{Ph} was also crystallized, and its structure was compared with the original structure (Fig. 7C). This study identified the conformational changes required to bring about the formation of the crosslinks and also suggested a mechanism for the transport process and how this process can lead to channel activation (Reyes et al., 2009). Briefly, the three transport domains (consisting of TM3, TM6, TM7 and TM8 and HP1 and HP2 from each protomer) move as three separate units through a rigid trimerization scaffold. TM2 is part of the scaffold, whilst HP2 is part of the transport domain. It would appear that the sliding movement of the transport domain relative to the rigid trimerization scaffold allows chloride ions to pass through the gap between the two functional domains (Vandenberg et al., 2008). Further mutagenesis will be required to verify this proposal. This series of experiments starting with mutagenesis, followed by crystallography, further mutagenesis and then further crystallography, which will also be followed up by further mutagenesis, highlights how the two approaches to understanding structure and function relationships can complement one another and provoke new ideas and concepts in protein function.

3.5 Substrate affinity and K^+ ion coupling in EAAT1

For the last section of this chapter, we will focus on an example of how mutagenesis approaches have been used to understand substrate and ion binding properties of the glutamate transporter family. Many of the residues that have been implicated in substrate and ion binding/translocation (Bendahan et al., 2000; Kavanaugh et al., 1997; Vandenberg et al., 1995) and chloride permeation (Ryan et al., 2004) are conserved throughout the glutamate transporter family. In particular, the carboxy-termini of both the EAATs and Glt_{Ph} are highly conserved and contain the substrate and Na^+ binding sites. Despite their significant amino acid identity, the EAATs and Glt_{Ph} display several functional differences. The EAATs transport aspartate and glutamate with similar affinity, while Glt_{Ph} is selective for aspartate over glutamate. In addition, Glt_{Ph} transport is not coupled to the co-transport of H^+ or the counter-transport of K^+ (Boudker et al., 2007; Ryan et al., 2009). Examination of the amino acid sequences of the substrate binding site of the EAATs and Glt_{Ph} does not reveal any residues that can clearly account for the differences observed in substrate selectivity or affinity. However, an arginine residue is in close proximity to the substrate binding site of both the EAATs and Glt_{Ph}, but it is located in TM8 in the EAATs and in HP1 of Glt_{Ph} (Fig 1B). The aim of our study was to investigate the functional effect of the location of a positively charged arginine residue in two members of the glutamate transporter family, EAAT1 and Glt_{Ph}.

In order to examine the role of this arginine residue, two double mutant transporters were produced. In EAAT1 the arginine residue was moved from TM8 to HP1 (EAAT1S363R/R477M), and the reverse double mutation was introduced into the gene for Glt_{Ph} (Glt_{Ph}R276S/M395R). Switching the arginine residue from TM8 to HP1 in EAAT1 had

no effect on substrate selectivity, but it did increase affinity for both glutamate and aspartate and abolished K^+ coupling. The apparent affinity for both L-glutamate and L-aspartate was increased ~130 fold, and it was similar to the affinity of L-aspartate in Glt_{Ph} (Ryan et al., 2009). The counter-transport of one K^+ ion per transport cycle is thought to be important for the relocation of the EAATs to the outward-facing state. The movement of an arginine residue from TM8 to HP1 has potentially slowed the return of the empty transporter to the extracellular facing side, thus contributing to the decrease in observed affinity values. In contrast, the inverse changes in Glt_{Ph} (Glt_{Ph}R276S/M395R) resulted in a functional transporter that has a ~4-fold reduction in the affinity for aspartate compared to wild type. The substitutions did not affect substrate selectivity or introduce K^+ dependence.

The crystal structure of Glt_{Ph} reveals that the backbone carbonyl group of the arginine residue in HP1 forms a direct contact with the substrate. However, our mutagenesis studies suggest that it is the side chain that is influencing transport properties. A possible explanation is that the conformation of the HP1 loop region and also the proximal TM8 is influenced by the arginine side chain and neighbouring residues. Thus, mutating this arginine may influence the conformation of the backbone carbonyl group, which in turn may influence substrate affinity.

The movement of K^+ ions through the transporter is likely to rely upon multiple conformational changes and interactions. Disruption of any of these interactions via a mutation is liable to result in loss of K^+ coupling. However, to introduce K^+ coupling will require multiple mutations. This may explain why the double mutation is sufficient to abolish K^+ coupling in EAAT1, but not introduce it into Glt_{Ph}.

4. Conclusion

Directed mutagenesis has been particularly useful in understanding the structure and function of mammalian membrane proteins. In this chapter we have outlined our approach to structure-activity studies of neurotransmitter transporters in the solute carrier (SLC) families, SLC1 and SLC6. We have used examples from our work on the excitatory amino acid transporters (EAATs), the archaeal aspartate transporter (Glt_{Ph}), glycine transporters (GLYTs) and the prokaryotic leucine transporter ($LeuT_{Aa}$).

5. Acknowledgments

We are grateful for the technical assistance of Audra McKinzie, Cheryl Handford and Marietta Salim. Our research group is funded by the Australian National Health and Medical Research Council and the Australian Research Council.

6. References

Aragon C. & Lopez-Corcuera B. (2003). Structure, function and regulation of glycine neurotransporters. *European Journal of Pharmacology* 479(1-3): 249-262.

Arriza J., Kavanaugh M., Fairman W., Wu Y., Murdoch G., North R. & Amara S. (1993). Cloning and expression of a human neutral amino acid transporter with structural similarity to the glutamate transporter gene family. *Journal of Biological Chemistry* 268(21): 15329.

Aubrey K.R. & Vandenberg R.J. (2001). N[3-(4'-fluorophenyl)-3-(4'-phenylphenoxy)propyl]sarcosine (NFPS) is a selective persistent inhibitor of glycine transport. *British Journal of Pharmacology* 134(7): 1429-1436.

Bartholomaus I., Milan-Lobo L., Nicke A., Dutertre S., Hastrup H., Jha A., Gether U., Sitte H.H., Betz H. & Eulenburg V. (2008). Glycine transporter dimers: evidence for occurrence in the plasma membrane. *Journal of Biological Chemistry* 283(16): 10978-10991.

Bendahan A., Armon A., Madani N., Kavanaugh M. & Kanner B. (2000). Arginine 447 plays a pivotal role in substrate interactions in a neuronal glutamate transporter. *Journal of Biological Chemistry* 275(48): 37436.

Boudker O., Ryan R., Yernool D., Shimamoto K. & Gouaux E. (2007). Coupling substrate and ion binding to extracellular gate of a sodium-dependent aspartate transporter. *Nature* 445(7126): 387-393.

Dohi T., Morita K., Kitayama T., Motoyama N. & Morioka N. (2009). Glycine transporter inhibitors as a novel drug discovery strategy for neuropathic pain. *Pharmacology and Therapeutics* 123(1): 54-79.

Edington A.R., McKinzie A.A., Reynolds A.J., Kassiou M., Ryan R.M. & Vandenberg R.J. (2009). Extracellular loops 2 and 4 of GLYT2 are required for N-arachidonylglycine inhibition of glycine transport. *Journal of Biological Chemistry* 284(52): 36424-36430.

Fairman W.A., Vandenberg R.J., Arriza J.L., Kavanaugh M.P. & Amara S.G. (1995). An excitatory amino-acid transporter with properties of a ligand-gated chloride channel. *Nature* 375(6532): 599-603.

Guastella J., Nelson N., Nelson H., Czyzyk L., Keynan S., Miedel M.C., Davidson N., Lester H.A. & Kanner B.I. (1990). Cloning and expression of a rat brain GABA transporter. *Science* 249(4974): 1303-1306.

Horiuchi M., Nicke A., Gomeza J., Aschrafi A., Schmalzing G. & Betz H. (2001). Surface-localized glycine transporters 1 and 2 function as monomeric proteins in Xenopus oocytes. *Proc Natl Acad Sci U S A* 98(4): 1448-1453.

Ju P., Aubrey K.R. & Vandenberg R.J. (2004). Zn2+ inhibits glycine transport by glycine transporter subtype 1b. *Journal of Biological Chemistry* 279(22): 22983-22991.

Kanai Y. & Hediger M. (2004). The glutamate/neutral amino acid transporter family SLC1: molecular, physiological and pharmacological aspects. *Pflügers Archiv European Journal of Physiology* 447(5): 469-479.

Kavanaugh M., Bendahan A., Zerangue N., Zhang Y. & Kanner B. (1997). Mutation of an amino acid residue influencing potassium coupling in the glutamate transporter GLT-1 induces obligate exchange. *Journal of Biological Chemistry* 272(3): 1703.

Lopez-Corcuera B., Alcantara R., Vazquez J. & Aragon C. (1993). Hydrodynamic properties and immunological identification of the sodium- and chloride-coupled glycine transporter. *J Biol Chem* 268(3): 2239-2243.

Reyes N., Ginter C. & Boudker O. (2009). Transport mechanism of a bacterial homologue of glutamate transporters. *Nature* 462(7275): 880-885.

Ryan R.M., Compton E.L. & Mindell J.A. (2009). Functional characterization of a Na+-dependent aspartate transporter from Pyrococcus horikoshii. *Journal of Biological Chemistry* 284(26): 17540-17548.

Ryan R.M. & Mindell J.A. (2007). The uncoupled chloride conductance of a bacterial glutamate transporter homolog. *Nature Structural and Molecular Biology* 14(5): 365-371.

Ryan R.M., Mitrovic A.D. & Vandenberg R.J. (2004). The chloride permeation pathway of a glutamate transporter and its proximity to the glutamate translocation pathway. *Journal of Biological Chemistry* 279(20): 20742-20751.

Ryan R.M. & Vandenberg R.J. (2002). Distinct conformational states mediate the transport and anion channel properties of the glutamate transporter EAAT-1. *Journal of Biological Chemistry* 277(16): 13494-13500.

Schrodinger L. (2010). The PyMOL Molecular Graphics System, Version 1.3r1.

Shevchuk N.A., Bryksin A.V., Nusinovich Y.A., Cabello F.C., Sutherland M. & Ladisch S. (2004). Construction of long DNA molecules using long PCR-based fusion of several fragments simultaneously. *Nucleic Acids Research* 32(2): e19.

Singh S.K., Piscitelli C.L., Yamashita A. & Gouaux E. (2008). A competitive inhibitor traps LeuT in an open-to-out conformation. *Science* 322(5908): 1655-1661.

Singh S.K., Yamashita A. & Gouaux E. (2007). Antidepressant binding site in a bacterial homologue of neurotransmitter transporters. *Nature* 448(7156): 952-956.

Slotboom D.J., Konings W.N. & Lolkema J.S. (1999). Structural features of the glutamate transporter family. *Microbiology and Molecular Biology Reviews* 63(2): 293-307.

Succar R., Mitchell V.A. & Vaughan C.W. (2007). Actions of N-arachidonyl-glycine in a rat inflammatory pain model. *Molecular Pain* 3: 24.

Supplisson S. & Bergman C. (1997). Control of NMDA receptor activation by a glycine transporter co-expressed in Xenopus oocytes. *Journal of Neuroscience* 17(12): 4580-4590.

Sur C. & Kinney G.G. (2004). The therapeutic potential of glycine transporter-1 inhibitors. *Expert Opinion on Investigational Drugs* 13(5): 515-521.

Vandenberg R.J., Arriza J.L., Amara S.G. & Kavanaugh M.P. (1995). Constitutive ion fluxes and substrate binding domains of human glutamate transporters. *Journal of Biological Chemistry* 270(30): 17668-17671.

Vandenberg R.J., Huang S. & Ryan R.M. (2008). Slips, leaks and channels in glutamate transporters. *Channels (Austin)* 2(1): 51-58.

Vandenberg R.J., Shaddick K. & Ju P. (2007). Molecular basis for substrate discrimination by glycine transporters. *Journal of Biological Chemistry* 282(19): 14447-14453.

Vuong L.A., Mitchell V.A. & Vaughan C.W. (2008). Actions of N-arachidonyl-glycine in a rat neuropathic pain model. *Neuropharmacology* 54(1): 189-193.

Wadiche J.I., Amara S.G. & Kavanaugh M.P. (1995). Ion fluxes associated with excitatory amino acid transport. *Neuron* 15(3): 721-728.

Wiles A.L., Pearlman R.J., Rosvall M., Aubrey K.R. & Vandenberg R.J. (2006). N-Arachidonyl-glycine inhibits the glycine transporter, GLYT2a. *Journal of Neurochemistry* 99(3): 781-786.

Yamashita A., Singh S.K., Kawate T., Jin Y. & Gouaux E. (2005). Crystal structure of a bacterial homologue of Na+/Cl--dependent neurotransmitter transporters. *Nature* 437(7056): 215-223.

Yernool D., Boudker O., Jin Y. & Gouaux E. (2004). Structure of a glutamate transporter homologue from Pyrococcus horikoshii. *Nature* 431(7010): 811-818.

Zerangue N. & Kavanaugh M. (1996). Flux coupling in a neuronal glutamate transporter. *Nature* 383(6601): 634-637.

IntechOpen